

OTHER CONDENSED MATTER

Magnetotransport Properties of Novel Semiconducting and Mesoscopic Structures

Bleiweiss, M., Univ. of South Carolina,
Physics and Astronomy
Datta, T., Univ. of South Carolina,
Physics and Astronomy

We are currently studying the interaction between magnetic fields and transport electrons in a number of solid materials, in particular, magnetoresistance (MR), Hall effects, and Shubnikov-de Haas (SdH) oscillations. The primary materials of interest are $\text{La}_{1-x}\text{A}_x\text{MnO}_3$ (where A is either Ca or Sr), perovskites, and synthetic opal structures that have been infiltrated with bismuth or carbon.

The manganate perovskites have the interesting property that they exhibit an extremely large negative MR, termed colossal magnetoresistance (CMR). This phenomenon has attracted a great deal of attention in the past several years due to the possible technological applications, as well as providing insight into exactly how magnetic fields interact with the transport electrons in these solids. The CMR effect typically occurs in the region near the Curie temperature, where the material undergoes a magnetic phase transition from a paramagnetic to ferromagnetic state. That is, a change in the conductivity from insulator to metal accompanies the change in magnetic ordering; so that, the magnetically disordered state is associated with insulating or semiconducting transport and the magnetically ordered ferromagnetic phase is associated with metallic conduction. This type of metal-insulator transition is unusual and poorly understood. Several theories attempting to explain CMR have been proposed and account for some aspects of CMR, but they are, at the very least, incomplete.¹ Further study is needed to determine which of these models, if any, is better in explaining the mechanism for CMR.

The manganate samples we are using exhibit an unusual low field positive MR, however, at high fields show the more common negative MR. We have also noted a change in the Hall properties depending on whether we are above or below the Curie temperature. The study of these effects, as well as high magnetic field transport measurements are necessary to distinguish between the mechanisms proposed to be the cause of CMR.

The artificial opal structures are comprised of silica spheres of uniform size in a face centered, close packed cubic lattice. This leads to regularly spaced and shaped voids between the spheres of two types, tetrahedral and octahedral. They have approximate sizes on the order of 100 nm for the tetrahedral voids and 35 nm for the octahedral ones. Filling these voids provides a regular, three-dimensional structure composed of nanoscale regions.

The first of these mesoscopic structures we are studying consists of high purity bismuth infiltrated into the interstitial regions of synthetic opals. Bismuth is a well-known semimetal whose electronic properties are very different from common metals. Because of these properties, bismuth thin films have been used to study quantum effects, and the influence of reduced dimensionality has been seen in samples with dimensions on the order of 100 nm.² Finite size effects in these systems have led to enhanced MR and SdH oscillations.^{3,4} SdH oscillations, like the de Haas van Alphen effect, can only be seen using high magnetic fields. Localization effects due to reduced dimensionality have been seen in our samples. These samples also exhibit an unusual Hall behavior in which there is a field induced change in the majority carrier. That is, upon application of a large enough magnetic field, the majority carrier changes.

The carbon inverse opal structures also exhibit unusual properties due to finite size effects, such as SdH oscillations and possible Quantum Hall effects. Extremely high magnetic fields are required in order to observe both of these effects.

- ¹ Matl, P., *et al.*, Phys. Rev. B, **57**, 10248 (1998).
² Heremans, J., *et al.*, Phys. Rev. B, **58**, R10091 (1998).
³ Liu, K., *et al.*, Phys. Rev. B, **58**, R14681 (1998).
⁴ Zhang, Z., *et al.*, Appl. Phys Lett., **73**, 1589 (1998).

Novel Amplitude Modulation Effects in Graphite Particle Orbits in Magnetic Levitation Under Ambient Air and Vacuum Conditions ▽IHRP▲

Brooks, J.S., NHMFL
 Cothorn, J., NHMFL
 Rutel, I., NHMFL
 Summerlin, D., Mt. Dora High School
 Marsceill, A., Pine Crest High School

We have investigated many examples of the dynamics and configurations of granular materials, taken either as isolated particles, or in interacting assemblies, under unique conditions where the gravitational force is balanced by a diamagnetic force. The associated phenomena has been the subject of several publications^{1,2,3} and also a previous NHMFL report.⁴ One curious aspect of the dynamic motion of graphite-composite particles is their highly irregular motion when perturbed from their equilibrium position in the magnet. The trajectory analysis for one such orbit is shown in Fig. 1 for a particle moving in the field of a 20 T wide bore magnet in the magnetic levitation balance condition. The over frame of Fig. 1a shows the first return plot of the particle trajectory (depicted in the lower right quadrant). The first return points are derived from the Poincaré section (open circles in the trajectory plot). The scatter in the first return plot (which is commonly used as a measure of chaotic motion) represents a high degree of irregular motion in the trajectory. The Fourier transform of the motion (depicted in the upper right quadrant) shows the presence of two harmonic motion frequencies.

One of the most interesting outcomes of the experiments in Fig. 1a is the amplitude modulation (AM) effect shown in Fig. 1b. The total mechanical energy of the single particle system has been computed by assuming the simple two-dimensional harmonic oscillator form $2E/m=v^2+cr^2$, where c is a constant which involves the ratio of the effective

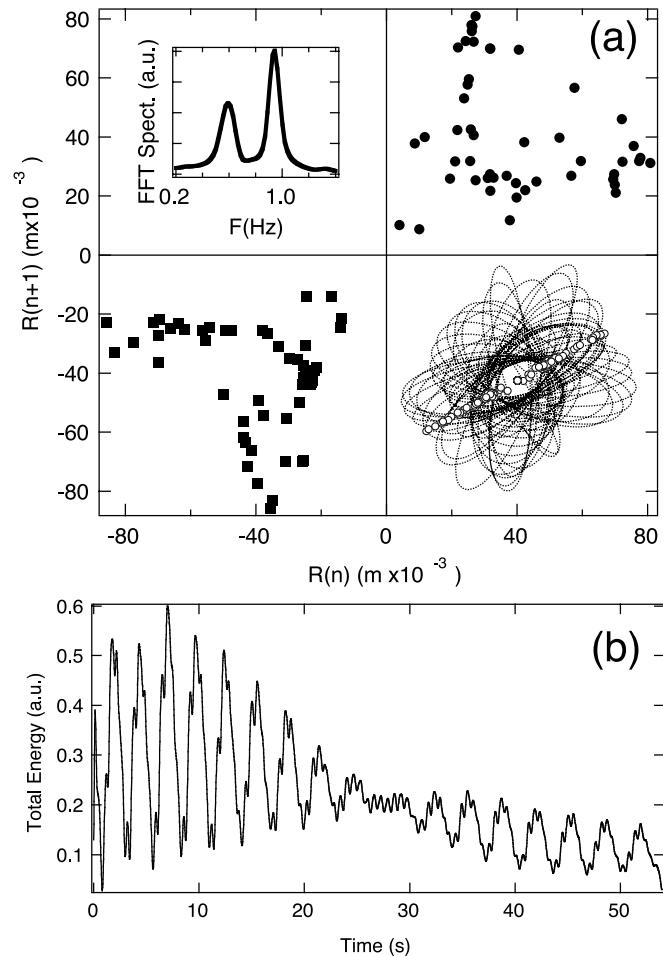


Figure 1. Trajectory analysis of a 1.1 cm diameter graphite-epoxy composite sphere (a) First return plot of position R_n of the particle for the Poincaré section $Y=X$ (open circles) determined from the trajectory shown in the lower right inset. Solid circles and squares in the main panel are the exit and entry points, respectively, of the Poincaré section. The upper left inset is the Fourier transform of the X motion. (b) Time dependence of total mechanical energy. The large oscillations are due to the AM effect on the total energy. The smaller, higher frequency oscillations result from residual differences between the kinetic and potential energy computations.

constant to the mass. (The radial restoring force follows an approximate Hooke's law relation, i.e., linear in r , out to about 0.06 m as checked both by experiment and computation). Physically, the AM effect represents the variation of the amplitude (at about 0.2 Hz), and therefore the total energy, of the two-dimensional harmonic oscillator system which is oscillating at distinctly different frequencies shown in the Fourier transform.

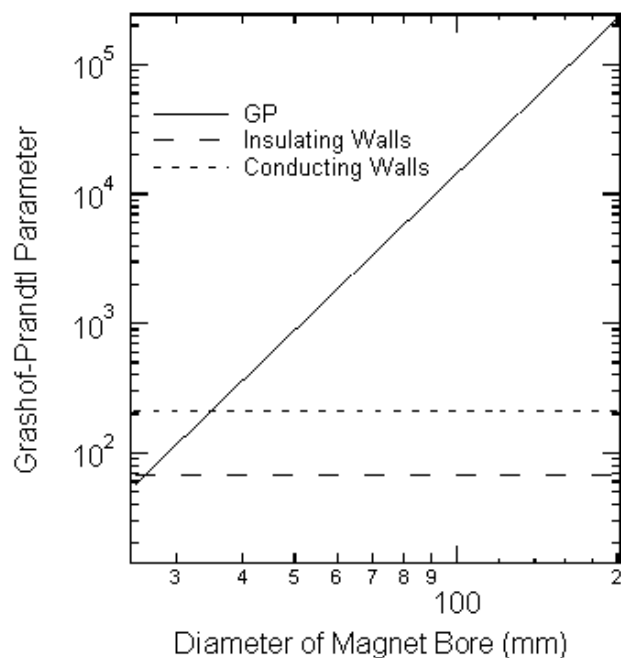


Figure 2. Estimates, from Ref. 5, of the onset of air convection in the water-cooled resistive magnets at the NHMFL, in terms of the Grashof-Prandtl parameter vs. magnet bore radius. Since the walls of the 33 bore magnets are conducting, even these magnets will sustain convective currents.

We originally expected that the large fluctuations in the total mechanical energy seen in Fig. 1b represented the presence of convection currents that can be present in the resistive magnet bore. They most likely arise from the temperature gradient (of order 10°C over a meter), since the magnets are water-cooled by uniaxial flow. To estimate the onset of convection, we computed the Grashof-Prandtl number⁵ vs. magnet bore in the water-cooled resistive magnet environment, as shown in Fig. 2. Clearly, convection should occur in all cases, and especially in the wide bore magnet of 190 mm diameter.

To check directly the role of air convection on the trajectory, two of the authors (Marsceill and Summerlin, from the Young Scholars Program) built a transparent vacuum chamber which could be placed inside the magnet. The chamber had a manipulator to excite the trajectories of levitating objects, as shown in Fig. 3. The results of one of the vacuum experiments, one of which is indicated in Fig. 4, showed two important aspects of the anomalous motion originally identified in Fig. 1: (a) the effect of the air is mainly to attenuate the motion, i.e., the

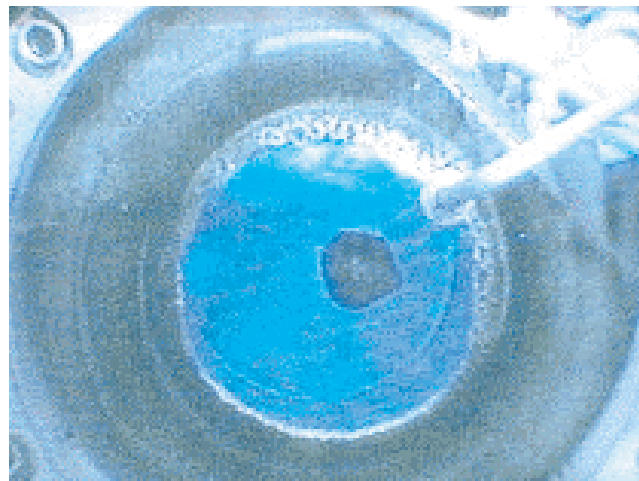


Figure 3. Picture of a graphite object levitating in a transparent, evacuated chamber in the 190 mm bore, 20 T magnet at the NHMFL.

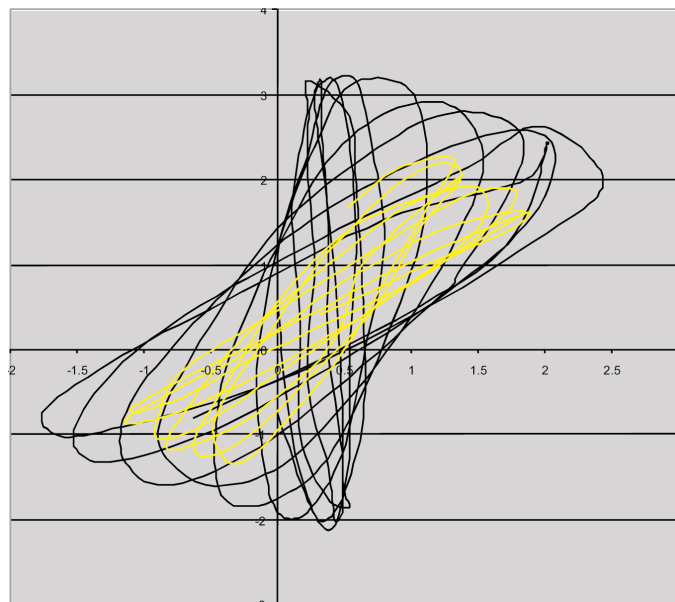


Figure 4. Digitized trajectories for motion in air (smaller amplitude trajectory) and in vacuum (larger amplitude trajectory). The trajectory in vacuum displays the same irregular AM motion as do trajectories in air, but with less attenuation.

total energy decreases with time due to air resistance, as is observed; (b) in contrast to our expectations concerning air convection, *the irregular motion of the particles remained, even in a vacuum.*

Given the results described above, we must now speculate that the irregular, AM motion is the result of electromagnetic effects which may arise from fluctuations in the magnetic field with time.

These are certainly small, but may be comparable to the equally small energy scale of the magnetic levitation condition. The coupling could be due to the conducting nature of the graphite systems we have investigated. More work is necessary to fully understand these novel dynamic effects, including the investigation of non-conducting particles under similar conditions.

Acknowledgements: The authors acknowledge support from IHRP/NHMFL 5033, NSF-DMR 95-10427 and 99-71474 (JSB). The NHMFL is supported through a cooperative agreement between the State of Florida and the NSF through NSF-DMR-95-27035.

¹ Brooks, J.S., *et al.*, J. Appl. Phys., **87**, 6194 (2000).

² Brooks, J.S., *et al.*, RHMFL-Porto, and Physica B, in press.

³ Brooks, J.S., *et al.*, ICM-Recife, and Physica B, in press.

⁴ Brooks, J.S., *et al.*, 1999 NHMFL Annual Research Review, 165-166 (1999).

⁵ Landau, L.D., *et al.*, Fluid Mechanics, 212-213 (1959).

The Study of Ultrafast Structural Dynamics on a Femtosecond Timescale with Time-Resolved Electron Diffraction

Cao, J., NHMFL/FSU, Physics

Understanding the structural dynamics of materials on the fundamental time scale for atomic motion represents an important frontier in scientific research. Many processes in nature, such as phase transitions, surface processes, chemical and biological reactions, are ultimately driven by the motion of atoms on the time scale of one vibrational period (~100 fs to 1 ps).

Our research is focused on the development of time-resolved electron diffraction for direct observation of these structural dynamics in real time on a femtosecond time scale. We are finishing the initial stage of research on developing a femtosecond electron diffraction (FED) instrument. Our FED contains five major components: an amplified sub-50 fs laser system, a home-made fs electron gun, a customized sample holder, a high quality diffraction

imaging system, and a streak camera. We expect that the FED will achieve ~500 fs overall temporal resolution and sufficient signal-to-noise ratio, and is capable of recording snapshots of clear diffraction pattern with single fs electron pulses.

The subsequent research will be centered on the investigation of the dynamics of structural phase transitions with FED in several prototypical systems. They include: (1) single crystal metal films (Au, Ni and Al); (2) poly-crystalline and amorphous metal samples; (3) the mono-atomic nano-particles; and (4) colossal magnetoresistance materials. The objectives of these studies are to gain a fundamental understanding on how the electron, spin, and lattice interactions affect the structural dynamics and associated physical properties in solids. It will be the first direct study of structural dynamics with fs time-resolution, based upon recording the snapshots of full diffraction images of transient structures, rather than recording only a single specific diffraction spot or line.

High Field NMR Studies of Density Waves in $\text{Rb}_{0.3}\text{MoO}_3$ and $(\text{TMTSF})_2\text{PF}_6$

Clark, W.G., Univ. of California, Los Angeles,
Physics and Astronomy

Vonlanthen, P., UCLA, Physics and Astronomy

Tanaka, K.B., UCLA, Physics and Astronomy

Goto, A., UCLA, Physics and Astronomy

Alavi, B., UCLA, Physics and Astronomy

Kriza, G., SZFKI (Budapest)

Moulton, W.G., NHMFL

Kuhns, P., NHMFL

Reyes, A.P., NHMFL

For one project, we report measurements of the ^{85}Rb and ^{87}Rb spin-lattice relaxation rate ($1/T_1$) in the quasi one-dimensional material $\text{Rb}_{0.3}\text{MoO}_3$, which has a metal to charge-density-wave (CDW) transition at 182 K. The measurements, which cover the temperature (T) range 2 K-300 K, were done using 9 T at UCLA and 23 T in the Cell 7 resistive magnet at the NHMFL in Tallahassee. Figure 1 presents a selected set of measurements obtained in this work.

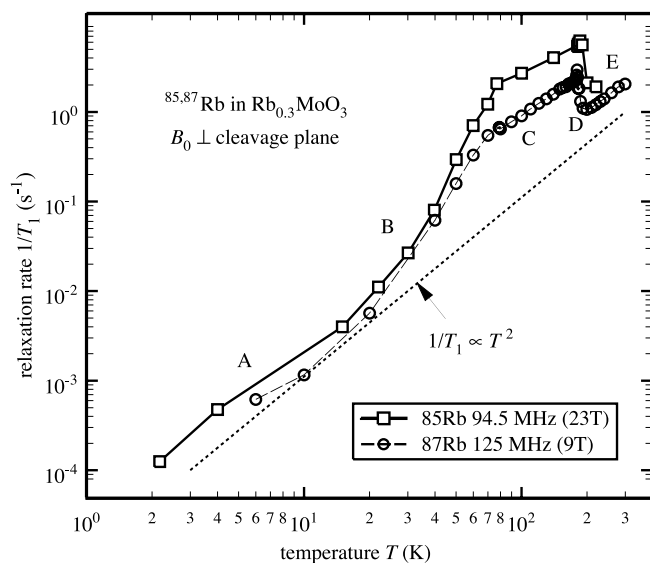


Figure 1. Spin-lattice relaxation rate of ^{85}Rb and ^{87}Rb as a function of temperature.

The static magnetic field (B_0) was aligned \perp to the cleavage plane. All of the measurements reported here were made on the central transition of the quadrupolar split spectrum of the 7-fold site. Five different temperature regimes are seen, which are indicated roughly by the letters on Fig. 1. They include the metallic regime somewhat above 182 K (E), the critical regime close to the CDW transition (D), the region (C) just below the transition, a low temperature regime (A) where $1/T_1 \propto T^2$, and a transitional region (B) between A and C.

The most surprising result is that the ratio of $1/T_1$ for the two isotopes shows that the dominant coupling for $1/T_1$ is quadrupolar over the entire temperature range; i.e., it is caused by charge fluctuations. Although this result is expected for regions A-D, in the metallic phase (E) it contradicts prior interpretations¹, which assumed that $1/T_1$ was from magnetic coupling to conduction electrons. We also find that there is a weak frequency dependence to $1/T_1$ in region B, but almost none in the others.

A second project uses ^1H spin-lattice relaxation rate ($1/T_1$) measurements to probe the spin-density-wave (SDW) fluctuations in the quasi 1-d system $(\text{TMTSF})_2\text{PF}_6$ up to 1.48 GHz (34.8 T) in the NHMFL hybrid magnet. This is, we believe, the highest frequency at which proton pulsed NMR measurements have ever been done. In the critical

regime above the SDW transition near 12 K, $1/T_1$ has no frequency dependence and the angular dependence of $1/T_1$ attributed to the spin-flop condition in the ordered phase is absent. These results indicate that amplitude fluctuations of the SDW drive $1/T_1$ in the critical regime and that the SDW critical fluctuation correlation time is 1×10^{-10} s. Somewhat below the transition, $1/T_1$ continues the decrease with increasing NMR frequency observed at lower frequencies. We attribute it to the power spectrum of the SDW phason fluctuations. The dependence of $1/T_1$ upon the field orientation in this phase reflects the spin-flop condition, but with parameters that are different from the expected ones.

Acknowledgements: The UCLA part of this work was supported by NSF Grants DMR-9705369 and DMR-0072524.

¹ Butaud, P., *et al.*, Journal de Physique, **51**, 59-89 (1990).

Magnetotransport in High Purity Bismuth Crystals ▀ IHRP ▀

Hebard, A.F., UF, Physics
 Maslov, D.M., UF, Physics
 Bompadre, S.G., UF, Physics
 Biagini, C., UF, Physics
 Derakhshan, J., West Virginia Univ.*

Magnetotransport has been investigated in high purity bismuth crystals in fields as high as 20 T and temperatures as low as 20 mK. This high B/T ratio permits observation of pronounced Shubnikov-de Haas oscillations (Fig. 1, top panel) up to fields where most of the carriers are in the lowest Landau level. The doublet splittings centered on each Shubnikov-de Haas oscillation exhibit a quadratic dependence on field and disappear before the last ($n = 1$) oscillation. The inset of Fig. 1 is a schematic of the energy levels showing the spin direction and identifications (n, v) of the order of oscillation n and the Landau level v . These observations allow us to conclude unambiguously that, for $v \leq 2$, the carriers are fully polarized and the g -factor for holes with the field in the trigonal direction is $35.3(4)$.¹

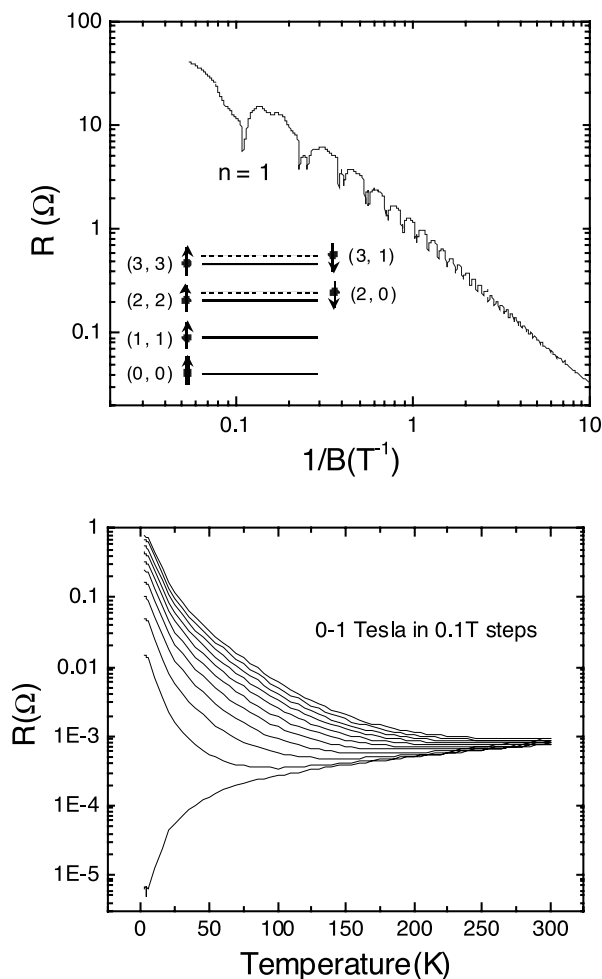


Figure 1. Longitudinal resistance plotted as a function of reciprocal field at 25 mK (top panel) and as a function of temperature at the indicated fields (bottom panel).

By sweeping the temperature in fixed fields (0 to 1.0 T in 0.1 T steps), the family of curves shown in Fig. 1 (bottom panel) is obtained. The magnetic field has a pronounced effect, giving a more than five-decade change in the resistance at 2 K. The magnetoresistivity data, $\rho(T,B) - \rho(T,0)$, are well described for two separate samples by the functional dependence, $A_1 B^{2-\eta} / (1 + A_2 T^2 B^{-\eta})$ where A_1 , A_2 , and η are constants. At low fields, the expected quadratic dependence, B^2 , is recovered. However, the quadratic temperature dependence in the denominator is inconsistent with the linear temperature dependence predicted by the two-band model for a perfectly compensated metal, thereby necessitating a reexamination of our understanding of the magnetoresistance of bismuth.

Acknowledgements: The authors would like to thank Professor R. Goodrich for the loan of high quality bismuth crystals, and the In-House Research Program of the NHMFL at Tallahassee for supporting this work.

* REU student at UF.

¹ Bompadre, S.G., *et al.*, submitted to Phys. Rev B (cond-mat/0006241).

Out-of-Plane Magnetoresistance of Sr_2RuO_4 ▽ IHRP ▲

Liu, Y., Penn State Univ., Physics
 Jin, R., Penn State Univ., Physics
 Nelson, K., Penn State Univ., Physics
 Lichtenberg, F., Augsburg Univ., Electronic Correlations and Magnetism

The enhancements of electronic specific heat and spin susceptibility of Sr_2RuO_4 are very similar to those found in ^3He , suggesting that is a strongly correlated system. Its in- and out-of-plane resistivities (ρ_{ab} and ρ_c , respectively) in the normal state of Sr_2RuO_4 follows a T^2 -dependence, characteristic of a Fermi liquid. Our measurements were focused on the normal-state magnetoresistance (MR) of superconducting Sr_2RuO_4 single crystals, which has been studied previously at relatively high temperatures¹ and in relatively low fields.¹ In this study, we measured out-of-plane resistance as a function of magnetic field, which was aligned both along and perpendicular to the current directions (corresponding to longitudinal and transverse MR).

Single crystals used in this study were grown by a floating-zone method. Resistance measurement shows a superconducting transition temperature (T_c) of 0.84 K. Four-point resistance measurements were carried out in a dilution refrigerator using a superconducting magnet. The temperature was monitored using a ruthenium oxide thermometer. The out-of-plane resistance measured at the base temperature (≈ 30 mK) and at 1.5 K is shown in Fig. 1, with field along the ab -plane and c -axis respectively. These results are consistent with

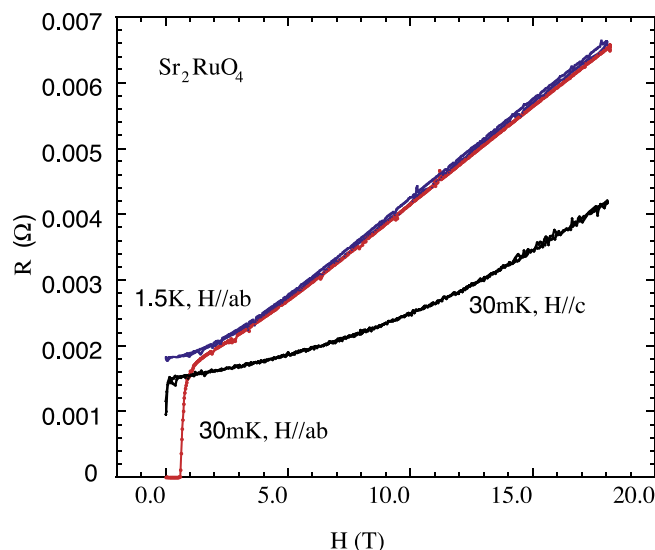


Figure 1. Out-of-plane resistance of Sr_2RuO_4 as a function of magnetic field. The temperatures and field orientations are indicated.

previous measurements in the overlapping parameter regimes.^{1,2}

Several interesting features can be identified. First, the transverse MR shows an unusual linear behavior, as previously found.² Second, no saturation was found for both longitudinal and transverse MR. The former has been noted previously for in-plane MR and explained in a spin pseudo gap picture.² The present experiment has information on the transport properties of Sr_2RuO_4 .

Acknowledgements: We would like to thank Scott Hannahs, Tim Murphy, and Eric Palm for help with the measurements. This work is supported by NSF (DMR-9974327) and the NHMFL.

¹ Hussey, N.E., *et al.*, Phys. Rev. B, **57**, 5505 (1998).

² Jin, R., *et al.*, Phys. Rev. B, **60**, 10418 (1999).

¹⁰⁹Ag NMR Study of Mobile Ions in the Glassy Fast Ionic Conductor $z\text{AgI} + (1-z)(0.525\text{Ag}_2\text{S} + 0.475(0.5\text{B}_2\text{S}_3 + 0.5\text{SiS}_2))$

Martin, S.W., Iowa State Univ., Materials Science and Engineering

Borsa, F., Iowa State Univ./Ames Laboratory, Materials Science and Engineering

Meyer, B., Iowa State Univ./Ames Laboratory, Materials Science and Engineering

Schrooten, J., Iowa State Univ., Materials Science and Engineering

The glass $0.525\text{Ag}_2\text{S} + 0.475(0.5\text{B}_2\text{S}_3 + 0.5\text{SiS}_2)$ was doped with silver iodide to form the $z=0.0, 0.1, 0.2, 0.3,$ and 0.4 compositions, where z is the molar fraction of AgI. These glasses possess an ability to decouple the silver ions from the structural relaxation of the glass. This decoupling gives rise to measured conductivities around 10^{-2} to 10^{-1} $(\text{Ohm}\cdot\text{cm})^{-1}$ at room temperature. As temperature is increased, it has been observed that a non-Arrhenius deviation from extrapolated room temperature values of the conductivity appears. The amount of deviation is heavily dependent upon the concentration of AgI doping.

Samples were prepared in an oxygen-free and water-free glove box. Fig. 1 shows the chemical shift spectra for the $z\text{AgI} + (1-z)(0.525\text{Ag}_2\text{S} + 0.475(0.5\text{B}_2\text{S}_3 + 0.5\text{GeS}_2))$ fast ion conducting glasses. These measurements were performed at room temperature using the 19.6 T superconducting magnet at the NHMFL. At $z=0.0$, one broad peak (A) appears at +180 ppm shift relative to the AgI reference. This single peak (A) shows that all of the Ag^+ ions, on average, see one homogeneous environment throughout the glass network. Upon adding AgI, the $z=0.1$ sample shows two new peaks (B & C). Peak (B) appears at +370ppm shift. This new peak (B) is adjoined to the peak (A) by a very broad peak (C) centered around +260 ppm. It should be noted that the intensity of peak (A) diminishes as more AgI is added. Upon further addition of AgI, $z=0.2$, peak (B) shift to lower ppm and broadens. Peak (C) also shifts to lower field. At the $z=0.4$ sample, a fourth peak (D) appears at 250 ppm.

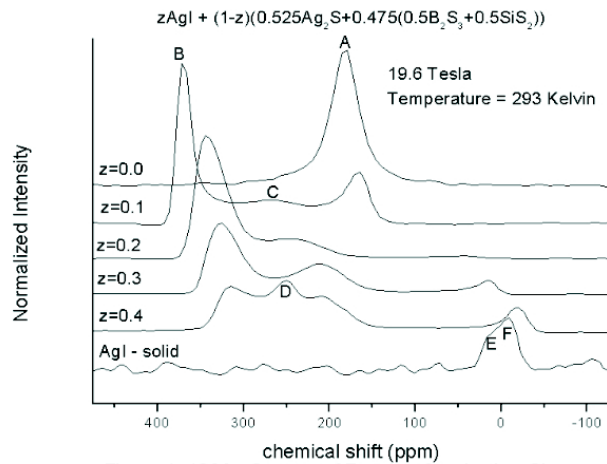


Figure 1. ^{109}Ag Spectra of Fast Ion Conducting Glasses

Figure 1. ^{109}Ag spectra of fast ion conducting glasses.

While all of the samples appeared to be glass forming, there is evidence of a separate silver iodide phase in the $z=0.3$, $z=0.4$, and possibly $z=0.2$ compositions. The AgI spectra is composed of two overlapped peaks (E and F) centered at 0 ppm. At temperatures below 150 °C, AgI possesses an hexagonal crystal structure.

Spin-lattice relaxation measurements showed that all of the peaks (A-F) shared a common T_1 value at room temperature. These measurements yielded T_1 values of 250 ms and 260 ms for the $z=0.0$ and $z=0.1$ samples respectively. $Z=0.2$ and $z=0.3$ had a T_1 of 330 ms. A T_1 of 315 ms was measured for $z=0.4$. For all five samples, the relaxation behavior was dominated by a single exponential behavior for over 90% of the recovered magnetization.

Future work will focus around temperature dependent spin-lattice relaxation measurements to further probe the ion hopping dynamics that occur in the non-Arrhenius regions of the conductivity.

Magnetically Induced Texture Changes in Zn-1.1% Al Alloy

Sheikh-Ali, A.D., NHMFL/FAMU-FSU College of Engineering and MARTECH

Garmestani, H., NHMFL/FAMU-FSU College of Engineering and MARTECH

It has been shown that magnetic field can affect or initiate grain boundary motion (migration) in bismuth bicrystals and coarse-grained polycrystals.^{1, 2} The magnetic driving force for boundary migration is produced by the difference in diamagnetic susceptibilities of neighboring grains. However, in most anisotropic diamagnetic materials this difference is significantly smaller than in bismuth. Therefore, magnetically induced boundary migration in these materials can be expected in the case of sufficiently high magnetic fields.

The objective of this project is to study texture changes in Zn-1.1%Al alloy during annealing under a strong magnetic field. Zn-1.1%Al alloy was prepared from pure metals (99.995% Zn and 99.99% Al). The casting was homogenized at 350° C for 60 hours. The ingot was rolled up to 95% reduction. After rolling, the alloy had a grain size of 3 μm . The experiments were carried out using a resistive, steady state 32 T magnet with 32 mm bore diameter. The samples of Zn-1.1% Al alloy were annealed at three different temperatures 130, 190, and 360° C in a magnetic field of 32 T. The field was applied in two different directions relative to the rolling direction of the samples. Magnetic strength, H, coincided with the rolling direction (RD) for one set of samples and was tilted at 20° about the transverse direction for the other one. The annealing time was 15 min. Fig. 1 shows the (0002) pole figures after rolling and after magnetic annealing. For all samples basal planes are tilted at 20° about the transverse direction (see Fig. 1a). Magnetic annealing of the first set of samples results in slight changes in the intensity of texture peaks (see Fig. 1b). For the second set of samples, the intensity of one peak increased markedly in contrast to the other (see Fig. 1c).

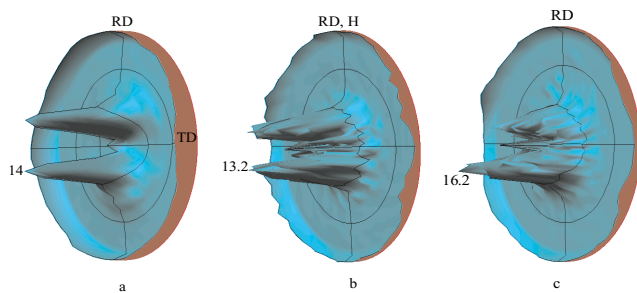


Figure 1. Pole figures of Zn-1.1%Al alloy. (a) After rolling, (b) after annealing at 360°C for 15 minutes, RD coincides with H, and (c) after annealing at 360°C for 15 minutes, RD tilted at 20° with respect to H.

These texture changes can be ascribed to the effect of magnetic field. When both peaks are tilted at the same angle to H there is no condition for preferential growth of grains belonging to one of these peaks. When basal planes become parallel to the field direction, the magnetic free energy of the respective grains, due to the anisotropy of magnetic susceptibility of Zn, tends to be at a minimum. The difference of the magnetic free energy in differently oriented grains exerts a driving force for the growth of grains having basal planes parallel to the field direction. Due to this additional driving force, these grains may grow faster than others and result in the increase of one of the texture peaks.

¹ Mullins, W.W., *Acta Metallurgica*, **4**, 421-432 (1956).

² Molodov, D.A., *et al.*, *Acta Materialia*, **46**, 5627-5632 (1998).

Tunneling Spectroscopy and Hall Effect Measurements on Gd_xSi_{1-x} and Y_xSi_{1-x}

▀ IHRP ▀

Teizer, W., Univ. of California, San Diego, Physics
Hellman, F., UCSD, Physics
Dynes, R.C., UCSD, Physics

We have extended tunneling spectroscopy measurements of amorphous Gd_xSi_{1-x} ¹ to higher magnetic fields. This allows for a determination of the density of states, $N(E)$, through the metal-insulator transition. Gd_xSi_{1-x} shows a strong negative magnetoresistance at low temperature² and can be

driven through the metal-insulator transition either by varying concentration x or by applying a magnetic field.³ For metallic Gd_xSi_{1-x} , at $H=0$, the conductance dI/dV across a $Gd_xSi_{1-x}/oxide/Pb$ tunnel junction is dominated by a sharp superconducting Pb gap edge and Pb phonons indicating the presence of single step quantum tunneling. As a small magnetic field ($H=1$ kOe) is applied, effects of the superconductivity of Pb disappear and at low voltages it is reasonable to approximate $dI/dV \sim N(E)$. We find that $N(E)$ increases with magnetic field. We observe a continuous transition from a regime where strong Coulomb correlations lead to a density of states $N(E) \sim N(0) + N_1 * E^y$ ($0.5 < y < 1$) to a regime where a soft gap appears, $N(E) \sim E^z$, $z > 1$ (See Fig.

1). On the metallic side of the metal-insulator transition, the density of states at zero bias, $N(0) \rightarrow 0$, approximately scales with the extrapolated $T=0$ transport conductivity σ_0 like $N(0) \sim \sigma_0^2$. The metal-insulator transition occurs when $N(0) \rightarrow 0$. Results on Al/oxide/ Gd_xSi_{1-x} tunnel junctions confirm these results and indicate that they are independent of the nature of the tunnel barrier.⁴

We have also extended Hall effect measurements in Gd_xSi_{1-x} and Y_xSi_{1-x} to higher magnetic fields. Y_xSi_{1-x} is a non-magnetic analog to Gd_xSi_{1-x} . The measurements show ordinary Hall effect in Y_xSi_{1-x} for $|H| < 180$ kOe. In Gd_xSi_{1-x} , a large anomalous contribution is seen for $|H| < 100$ kOe and behavior consistent with an ordinary Hall effect is seen for 100 kOe $< |H| < 180$ kOe. Usually, it is assumed that a change of carrier environment due to the alignment of magnetic moments leads to the anomalous Hall effect. Such an interpretation would suggest that the magnetic moments in Gd_xSi_{1-x} have reached saturated alignment at 100 kOe. In independent transport and tunneling measurements, however, a saturation of the conductivity and density of states is not observed up to $H=180$ kOe. This raises questions as to whether the anomalous Hall effect has a different origin than the large magnetoresistance and the changes in the density of states.

Acknowledgements: The authors would like to thank the NSF and the Air Force Office of Scientific Research for financial support.

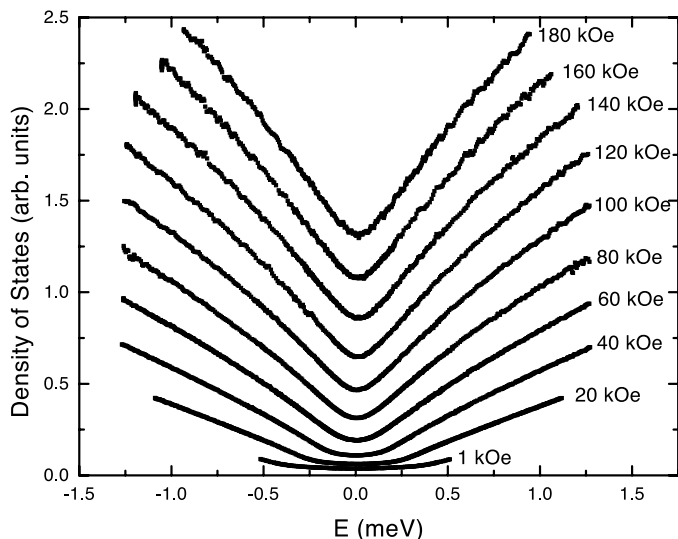


Figure 1. Density of states of Gd_xSi_x in the critical regime of the metal-insulator transition.

¹ Teizer, W., *et al.*, Phys. Rev. Lett., **85**, 848 (2000).

² Hellman, F., *et al.*, Phys. Rev. Lett., **77**, 4652 (1996). Xiong, P., *et al.*, Phys. Rev. B, **59**, 3929 (1999).

³ Teizer, W., *et al.*, Solid State Commun., **114**, 81 (2000).

⁴ Teizer, W., accepted in Proceedings of the 25th International Conference on the Physics of Semiconductors, January 2001.

Investigation of Sonoluminescence Under High Magnetic Fields

Young, J.B., Univ. of Chicago, James Franck Institute

Nelson, J.A., Univ. of Chicago, James Franck Institute

Kang, W., Univ. of Chicago, James Franck Institute

Sonoluminescence (SL) is an intriguing phenomenon in which gas bubbles are induced to emit light when excited by high intensity ultrasound.^{1,2} Although the phenomenon has been known for more than sixty years,³ the mechanism of light production is still a matter of active debate. The light is produced when a tiny ($\sim 5 \mu\text{m}$) bubble of gas trapped in water periodically collapses in response to the ultrasound. Some models of SL emission suggest significant densities of free charges may be present in the bubble during its collapse.^{4,5} Interactions between these free charges, if they exist, and external magnetic fields may provide a useful tool to probe the light production mechanism.⁶

In previous work conducted at NHMFL, we found that high magnetic fields do influence SL, causing the light emission to diminish parabolically with magnetic field.⁷ The light is extinguished when the field exceeds a parameter dependent threshold and further increase in the field can cause the bubble to dissolve. It is still unclear, however, whether these effects are due to magnetic coupling with the bubble interior, bubble wall, or exterior; it is possible that high field intensities could cause changes in the bubble's dynamics resulting in diminished SL emission as a secondary effect.

To clarify the nature of this magnetic field effect we have performed an experiment at NHMFL to measure the radius vs. time curves of SL bubbles for various values of magnetic field and sound intensity.⁸ The radius was found by measuring the intensity of laser light scattered by the SL bubble, which is proportional to the square of the bubble's radius. The curves, which have a time resolution of 20 ns, will be analyzed by fitting model equations of motion to the data. In this way, a comparison can be made with the well understood motion of bubbles in zero magnetic field and any significant deviations detected.

¹ Crum, L.A., Phys. Today, **47**, 22 (1994).

² Barber, B.P., *et al.*, Phys. Rev., **281**, 65 (1997).

³ Marinesko, N., *et al.*, C. R. Acad. Sci., **196**, 858 (1933).

⁴ Wu, C.C., *et al.*, Phys. Rev., **70**, 3424 (1993).

⁵ Moss, W.C., *et al.*, Phys. Rev. E, **59**, 2986 (1999).

⁶ Chou, T., *et al.*, Phys. Rev. Lett., **76**, 1549, (1996).

⁷ Young, J., *et al.*, Phys. Rev. Lett., **77**, 4816 (1996).

⁸ Young, J., *et al.*, unpublished.